

# **NIST Special Publication 260-133**

## **2001 Edition**

*Standard Reference Materials*<sup>®</sup>

### **Acetylene $^{12}\text{C}_2\text{H}_2$ Absorption Reference for 1510 nm to 1540 nm Wavelength Calibration—SRM 2517a**

Sarah L. Gilbert  
William C. Swann  
Optoelectronics Division  
Electronics and Electrical Engineering Laboratory  
Boulder, CO 80305-3328

Supersedes NIST Special Publication 260-133 (January 1998)



---

U.S. DEPARTMENT OF COMMERCE, *Donald L. Evans, Secretary*  
NATIONAL INSTITUTE OF STANDARDS AND TECHNOLOGY, *Karen H. Brown, Acting Director*

**Issued February 2001**

Certain commercial equipment, instruments, or materials are identified in this paper in order to specify the experimental procedure adequately. Such identification is not intended to imply recommendation or endorsement by the National Institute of Standards and Technology, nor is it intended to imply that the materials or equipment identified are necessarily the best available for the purpose.

**National Institute of Standards and Technology Special Publication 260-133 2001 ED**  
**Natl. Inst. Stand. Technol. Spec. Publ. 260-133 2001 ED, 29 pages (Feb. 2001)**  
**CODEN: NSPUE2**

**U.S. GOVERNMENT PRINTING OFFICE**  
**WASHINGTON: 2001**

---

For sale by the Superintendent of Documents, U.S. Government Printing Office  
Internet: [bookstore.gpo.gov](http://bookstore.gpo.gov) Phone: (202) 512-1800 Fax: (202) 512-2250  
Mail: Stop SSOP, Washington, DC 20402-0001

NIST Special Publication 260-133 (2001 Edition)

Standard Reference Materials:

**Acetylene  $^{12}\text{C}_2\text{H}_2$  Absorption Reference for 1510 nm to 1540 nm Wavelength Calibration – SRM 2517a**

Sarah L. Gilbert and William C. Swann

Optoelectronics Division  
Electronics and Electrical Engineering Laboratory  
National Institute of Standards and Technology  
Boulder, CO 80305-3328

**Abstract**

Standard Reference Material (SRM) 2517a is an optical-fiber-coupled wavelength reference based on the fundamental absorption lines of acetylene in the 1510 nm to 1540 nm region. The main difference between SRM 2517a and its predecessor, SRM 2517, is the use of lower pressure in the acetylene cell to produce narrower lines. Thus SRM 2517a extends the use to higher resolution and higher accuracy applications. The center wavelengths of 56 lines of the  $\nu_1 + \nu_3$  rotational-vibrational band of acetylene  $^{12}\text{C}_2\text{H}_2$  are certified for this SRM. Fifteen lines are certified with an uncertainty of 0.1 pm, two lines are certified with an uncertainty of 0.6 pm, and the remainder of the lines are certified with an uncertainty of 0.3 pm. This document describes SRM 2517a and details the uncertainty analysis.

Keywords: absorption; acetylene; molecular spectroscopy; optical fiber communications; pressure broadening; pressure shift; Standard Reference Material; wavelength calibration; wavelength division multiplexing; wavelength reference; wavelength standards; WDM

## 1. Introduction

Wavelength references are important in the 1500 nm region to support wavelength division multiplexed (WDM) optical fiber communication systems. In a WDM system, many wavelength channels are sent down the same fiber, thereby increasing the bandwidth of the system by the number of channels. If one channel's wavelength were to shift, crosstalk could occur between it and a neighboring channel. Wavelength references are needed to calibrate instruments that are used to characterize components and monitor the wavelengths of the channels.

Fundamental atomic or molecular absorption lines provide wavelength references that are very stable under changing environmental conditions, such as temperature and pressure variations or the presence of electromagnetic fields. There are several good molecular transitions in the 1500 nm region. The acetylene  $^{12}\text{C}_2\text{H}_2$   $\nu_1 + \nu_3$  rotational-vibrational combination band, shown in Fig. 1, contains about 50 strong lines between 1510 nm and 1540 nm. The corresponding band in  $^{13}\text{C}_2\text{H}_2$  extends from about 1520 nm to 1550 nm. Hydrogen cyanide also has a good spectrum, with lines between 1530 nm and 1565 nm for  $\text{H}^{13}\text{C}^{14}\text{N}$ . NIST has developed wavelength calibration Standard Reference Materials (SRM) based on acetylene (SRM 2517 [1]) and hydrogen cyanide (SRM 2519 [2]).

We have developed a new wavelength calibration standard, SRM 2517a. The main difference between SRM 2517a and its predecessor, SRM 2517, is the use of lower pressure in the acetylene cell to produce narrower lines. Thus SRM 2517a can be used in higher resolution and higher accuracy applications. This document describes SRM 2517a and summarizes the results of our uncertainty analysis.

Standard Reference Material 2517a is intended for wavelength calibration in the spectral region from 1510 nm to 1540 nm. It is a single-mode optical-fiber-coupled absorption cell containing acetylene ( $^{12}\text{C}_2\text{H}_2$ ) gas at a pressure of 6.7 kPa (50 Torr). The absorption path length is 5 cm and the absorption lines are about 7 pm wide. The cell is packaged in a small instrument box (approximately 24 cm long  $\times$  12.5 cm wide  $\times$  9 cm high) with two FC/PC fiber connectors for the input and output of a user-supplied light source. Acetylene has more than 50 accurately measured absorption lines in the 1500 nm wavelength region. This SRM can be used for high resolution applications, such as calibrating a narrowband tunable laser, or lower resolution applications, such as calibrating an optical spectrum analyzer. The certificate for SRM 2517a is presented in Appendix A. It includes the certified wavelength values, spectra, and instructions for use.

The vacuum wavelengths of the acetylene  $\nu_1 + \nu_3$  lines have been measured at very low pressure (1 Pa to 4 Pa, or equivalently 10 mTorr to 30 mTorr) with an uncertainty of about  $10^{-6}$  nm [3]. For a wavelength reference, the stability of the wavelength of each absorption line is a critical characteristic. The symmetric isotopic species of acetylene are particularly insensitive to external perturbation because they have no permanent dipole moment. The largest potential source of line shift is energy level shift caused by the interaction of the molecules during elastic collisions [4]. Commonly called the pressure shift, this shift depends linearly on the collision frequency. For wavelength calibration of instruments, it is often desirable to use a moderate or high pressure sample in order to increase the absorption depth. This results in pressure broadening and a slight pressure shift of the line centers. Our measurement of the pressure-

induced shift and broadening for 15 lines in the  $\nu_1 + \nu_3$  rotational-vibrational band of acetylene  $^{12}\text{C}_2\text{H}_2$  and evaluation of other shift mechanisms is described in Ref. 5 (Appendix B of this document).

The dominant sources of uncertainty for SRM 2517a are the pressure shift uncertainty and the line center measurement uncertainty. Section 2 gives the uncertainty analysis for the pressure shift adjustment. Section 3 details the uncertainty analysis for the line center measurement. We summarize the results in section 4.

## 2. Pressure Shift Adjustment

SRM 2517a uses acetylene  $^{12}\text{C}_2\text{H}_2$  gas at a pressure of  $6.7 \pm 1.3$  kPa ( $50 \pm 10$  Torr). We have made accurate measurements of the pressure shift for 15 lines in the  $\nu_1 + \nu_3$  rotational-vibrational band of acetylene  $^{12}\text{C}_2\text{H}_2$  [5]. For SRM 2517a, we derive the line centers by adding each line's pressure shift (at 6.7 kPa) to the low-pressure literature values [3]. Unless we specify otherwise, the uncertainties quoted in this document are expanded uncertainties using a coverage factor  $k = 2$  (i.e., our quoted uncertainty is  $\pm 2\sigma$ ).

Figure 2 shows the results of our pressure shift measurements. The pressure shift varies with line number and is largest for lines far from the band center (transitions between states with high rotational quantum number). In the R branch, the shift slope ranges from 0.008(2) pm/kPa for line R1 to 0.043(2) pm/kPa for line R27. The P branch shows less variation, with most lines having a slope near 0.017 pm/kPa. Table 1 summarizes our pressure shift slope measurements and the pressure shift derived for the SRM pressure of  $6.7 \pm 1.3$  kPa. Our uncertainty for the pressure shift of the 15 measured lines is dominated by the SRM cell pressure uncertainty. For the remainder of the lines in the band, we assign pressure shift values based on polynomial least-squares fitting to the data for each branch. The results for a quadratic fit of the R branch and a third-order polynomial fit for the P branch are:

$$\begin{aligned} Rshift(pm) &= 0.04 + 0.113n - 7.8 \times 10^{-5} n^2 \\ Pshift(pm) &= 0.10 + 0.0044n - 5.41 \times 10^{-4} n^2 + 1.93 \times 10^{-5} n^3, \end{aligned} \tag{1}$$

where  $n$  is the line number and the shift (in picometers) is for a pressure of 6.7 kPa. These values are tabulated in Table 2. The uncertainty of the fitted pressure shift is obtained by combining (in quadrature) the uncertainty of the fit and the uncertainty of the measured pressure shift.

## 3. Line Center Measurement Uncertainty

Wings of nearby lines can skew the shape of the line being measured and shift its apparent center. In addition to the strong lines of the  $\nu_1 + \nu_3$  band, there are a number of weak lines throughout the spectrum which are due to hot bands (transitions that are not out of the ground vibrational state) [6]. These small hot band lines overlap some of the main ( $\nu_1 + \nu_3$ ) lines and have a significant potential to shift their apparent line center. The 15 lines measured in Ref. 5 were selected on the basis of their relative isolation from nearby lines. We determined that our standard uncertainty ( $1\sigma$ ) for the measurement of these selected line centers was 0.05 pm [5].

Other lines in the band, however, will be assigned higher uncertainties due to the effect of nearby small lines. Our determination of this uncertainty is described below.

We first determined the approximate strengths of the nearby lines relative to the main lines of the  $\nu_1 + \nu_3$  band. Using high resolution spectra from Ref. 6 and our own scans using a tunable laser, we found that the strengths of most of these smaller lines are less than 15 % of the main  $\nu_1 + \nu_3$  lines. Lines R0, P1, and P18 are notable exceptions to this. Line R0 is weak, has significant hot band lines in the vicinity, and can be difficult to identify. For these reasons, we do not certify line R0. Lines P1 and P18 overlap hot band lines that have fractional strengths of about 20 % to 30 %; these two lines are certified with a higher uncertainty.

We modeled the effect of small nearby lines on the measurement of the main line centers by generating Lorentzian lineshapes and calculating the fitted line center for a line when it was summed with a second smaller nearby line. (The true lineshape is a Voigt profile [4], which is a convolution of a Lorentzian and Gaussian lineshape. Use of a Lorentzian function simplifies the modeling and yields a reasonable approximation of the effect.) We chose a Lorentzian full width at half maximum (FWHM) linewidth of 5 pm, which is close to the Lorentzian component of the linewidth at this pressure [5]. A second Lorentzian line with the same linewidth and a center wavelength slightly offset from the main line was summed with the modeled main line. We then used a least-squares fitting routine to determine the center of the main line. We restricted the fitting range to within  $\pm 5$  pm of the line center. This process was repeated using a variety of strengths and offsets for the second line. Figure 3 shows the results of the modeling for the conditions where the second line's fractional strength is 5, 10, 15, and 20 % of the main line. We found that the maximum shift of the main line always occurred when the second line was offset by about 3 pm from the main line center (about 60 % of the linewidth). Figure 4 plots the maximum shift of the main line versus the fractional strength of the second line. Since most of these smaller lines have fractional strengths of less than 15 %, we determine our uncertainty based on the maximum shift caused by a line with this fractional strength. As seen in Fig. 4, this shift is 0.25 pm. Assuming a rectangular distribution with upper and lower limits of  $\pm 0.25$  pm about the line center, this corresponds to a standard uncertainty ( $1\sigma$ ) of 0.14 pm ( $=0.25/\sqrt{3}$ ) [7]. For lines P1 and P18, where there are nearby lines with fractional strengths of up to 30 % of the main lines, we determine the uncertainty based on the maximum shift caused by a small line with a fractional strength of 30 %. From the data shown in Fig. 4, this maximum shift is 0.54 pm. Assuming a rectangular distribution with upper and lower limits of  $\pm 0.54$  pm about the line center, this corresponds to a standard uncertainty ( $1\sigma$ ) of 0.31 pm.

#### 4. Summary

Table 3 gives the SRM certified wavelengths for 56 lines of the  $\nu_1 + \nu_3$  band of acetylene  $^{12}\text{C}_2\text{H}_2$ . The uncertainties were obtained by combining the pressure shift uncertainty and the line center measurement uncertainty in quadrature. The 15 NIST-measured lines are certified with expanded uncertainties ( $2\sigma$ ) ranging from 0.10 pm to 0.12 pm. The remaining lines are assigned higher uncertainty, due primarily to the possible skewing of the lineshapes by small nearby lines. Thirty-nine of these lines are certified with an expanded uncertainty of 0.3 pm, and two lines are certified with an expanded uncertainty of 0.6 pm.

## 5. References

- [1] SRM 2517 used an acetylene pressure of 27 KPa (200 Torr). SRM 2517a (6.7 kPa pressure) replaces SRM 2517.
- [2] Gilbert, S.L.; Swann, W.C.; Wang, C.M. Hydrogen cyanide H<sup>13</sup>C<sup>14</sup>N absorption reference for 1530–1560 nm wavelength calibration – SRM 2519. Natl. Inst. Stand. Technol. Spec. Publ. 260-137; 1998.
- [3] Nakagawa, K.; Labachellerie, M.; Awaji, Y.; Kouroggi, M. Accurate optical frequency atlas of the 1.5- $\mu$ m bands of acetylene. J. Opt. Soc. Am. B 13: 2708-2714; 1996.
- [4] Demtröder, W. Laser Spectroscopy, second edition. Berlin, Heidelberg, New York: Springer-Verlag; 1996. pp. 67-82.
- [5] Swann, W.C.; Gilbert, S.L. Pressure-induced shift and broadening of 1510–1540-nm acetylene wavelength calibration lines. J. Opt. Soc. Am. B 17: 1263-1270; 2000. [Appendix B of this document].
- [6] Baldacci, A.; Ghersetti, S.; Rao, K.N. Interpretation of the acetylene spectrum at 1.5  $\mu$ m. J. Mol. Spectrosc. 68: 183-194; 1977; Guelachvili, G.; Rao, K.N. Handbook of Infrared Standards II. San Diego, CA: Academic Press, Inc.; 1993. pp. 564-571.
- [7] Taylor, B.N.; Kuyatt, C.E. Guidelines for Evaluating and Expressing the Uncertainty of NIST Measurement Results. Natl. Inst. Stand. Technol. Tech. Note 1297; 1994.

**Table 1. Pressure Shift Measurement Results**

Pressure shift results from Ref. 5 for the 15 measured lines of the  $\nu_1 + \nu_3$  band of acetylene  $^{12}\text{C}_2\text{H}_2$ . The uncertainties in the last digits of the values are indicated in parentheses. The uncertainties quoted are the expanded uncertainty using a coverage factor  $k = 2$  (i.e., our quoted uncertainty is  $\pm 2\sigma$ ).

Line	Pressure shift slope (pm/kPa)	Pressure shift, $P = 6.7 \pm 1.3$ kPa (pm)
R27	+ 0.043(2)	0.29(6)
R17	+ 0.032(2)	0.21(4)
R11	+ 0.023(2)	0.15(4)
R7	+ 0.017(2)	0.11(2)
R1	+ 0.008(2)	0.05(2)
P3	+ 0.016(2)	0.11(2)
P4	+ 0.017(2)	0.11(2)
P5	+ 0.017(2)	0.11(2)
P6	+ 0.016(3)	0.11(2)
P10	+ 0.017(2)	0.11(2)
P13	+ 0.016(2)	0.11(2)
P14	+ 0.016(2)	0.11(2)
P23	+ 0.023(2)	0.15(4)
P24	+ 0.024(3)	0.16(4)
P25	+ 0.026(2)	0.17(4)

**Table 2. Pressure Shift Fit Results**

Pressure shift values for a pressure of 6.7 kPa derived from polynomial fitting (Equation 1) of the data in Table 1.

R Branch	Shift (pm)	P Branch	Shift (pm)
29	0.30	1	0.10
28	0.30	2	0.11
27	0.29	3	0.11
26	0.28	4	0.11
25	0.27	5	0.11
24	0.27	6	0.11
23	0.26	7	0.11
22	0.25	8	0.11
21	0.24	9	0.11
20	0.23	10	0.11
19	0.23	11	0.11
18	0.22	12	0.11
17	0.21	13	0.11
16	0.20	14	0.11
15	0.19	15	0.11
14	0.18	16	0.11
13	0.17	17	0.11
12	0.16	18	0.12
11	0.15	19	0.12
10	0.15	20	0.13
9	0.14	21	0.13
8	0.13	22	0.14
7	0.11	23	0.15
6	0.11	24	0.16
5	0.09	25	0.17
4	0.08	26	0.19
3	0.07	27	0.20
2	0.06	28	0.22
1	0.05		
0	0.04		

**Table 3. Certified Wavelengths for SRM 2517a**

Literature values from Ref. 3 adjusted for the pressure shift listed in Table 2 due to the 6.7 kPa (50 Torr) cell pressure. These vacuum wavelengths of the  $\nu_1 + \nu_3$  band  $^{12}\text{C}_2\text{H}_2$  are certified with the uncertainty indicated in parentheses for the last digits. The uncertainties quoted are the expanded uncertainty using a coverage factor  $k = 2$  (i.e., our quoted uncertainty is  $\pm 2\sigma$ ). The lines in bold were accurately characterized by NIST [5] and have the lowest uncertainty.

R Branch	Wavelength (nm)	P Branch	Wavelength (nm)
29	1511.7304(3)	1	1525.7599(6)
28	1512.0884(3)	2	1526.3140(3)
<b>27</b>	<b>1512.45273(12)</b>	<b>3</b>	<b>1526.87435(10)</b>
26	1512.8232(3)	<b>4</b>	<b>1527.44114(10)</b>
25	1513.2000(3)	<b>5</b>	<b>1528.01432(10)</b>
24	1513.5832(3)	<b>6</b>	<b>1528.59390(10)</b>
23	1513.9726(3)	7	1529.1799(3)
22	1514.3683(3)	8	1529.7723(3)
21	1514.7703(3)	9	1530.3711(3)
20	1515.1786(3)	<b>10</b>	<b>1530.97627(10)</b>
19	1515.5932(3)	11	1531.5879(3)
18	1516.0141(3)	12	1532.2060(3)
<b>17</b>	<b>1516.44130(11)</b>	<b>13</b>	<b>1532.83045(10)</b>
16	1516.8747(3)	<b>14</b>	<b>1533.46136(10)</b>
15	1517.3145(3)	15	1534.0987(3)
14	1517.7606(3)	16	1534.7425(3)
13	1518.2131(3)	17	1535.3928(3)
12	1518.6718(3)	18	1536.0495(6)
<b>11</b>	<b>1519.13686(11)</b>	19	1536.7126(3)
10	1519.6083(3)	20	1537.3822(3)
9	1520.0860(3)	21	1538.0583(3)
8	1520.5700(3)	22	1538.7409(3)
<b>7</b>	<b>1521.06040(10)</b>	<b>23</b>	<b>1539.42992(11)</b>
6	1521.5572(3)	<b>24</b>	<b>1540.12544(11)</b>
5	1522.0603(3)	<b>25</b>	<b>1540.82744(11)</b>
4	1522.5697(3)	26	1541.5359(3)
3	1523.0855(3)	27	1542.2508(3)
2	1523.6077(3)		
<b>1</b>	<b>1524.13609(10)</b>		

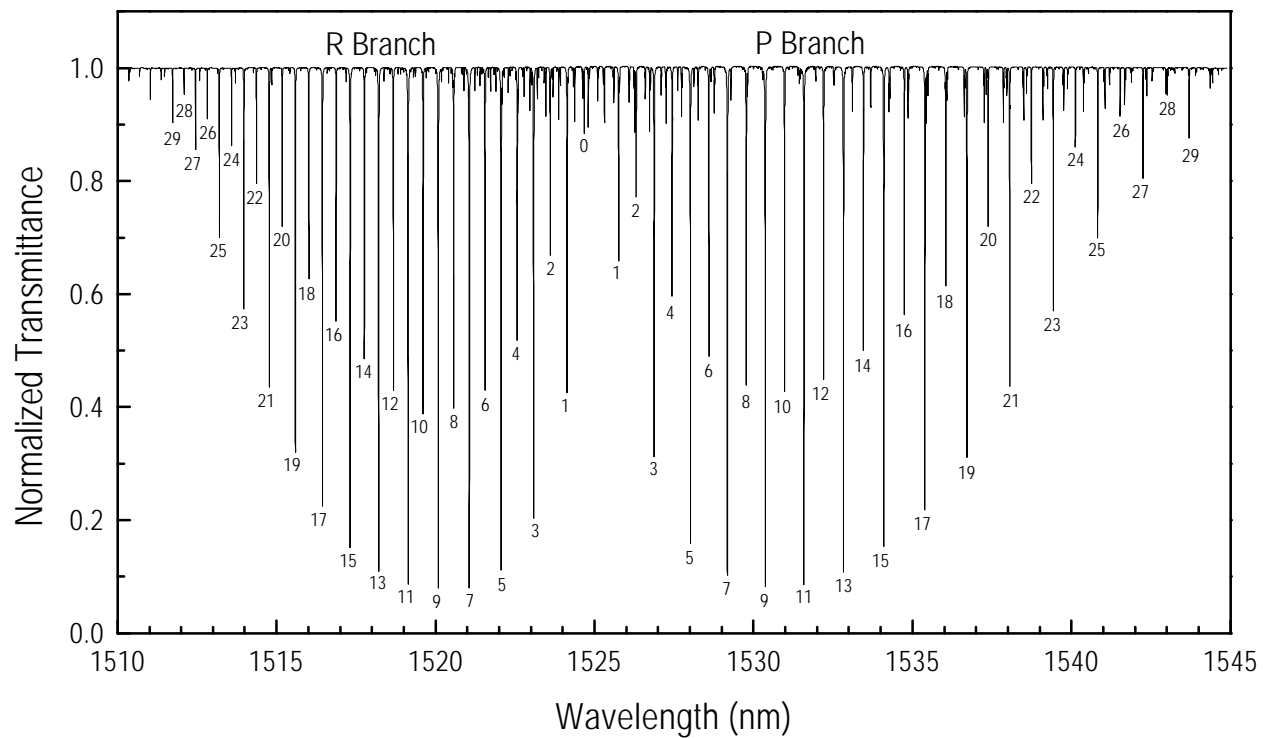


**Figure 1.** Spectrum of the acetylene  $^{12}\text{C}_2\text{H}_2$   $\nu_1 + \nu_3$  band obtained by scanning a tunable diode laser and measuring the laser power transmitted through a 5 cm long absorption cell filled to a pressure of 6.7 kPa (50 Torr).

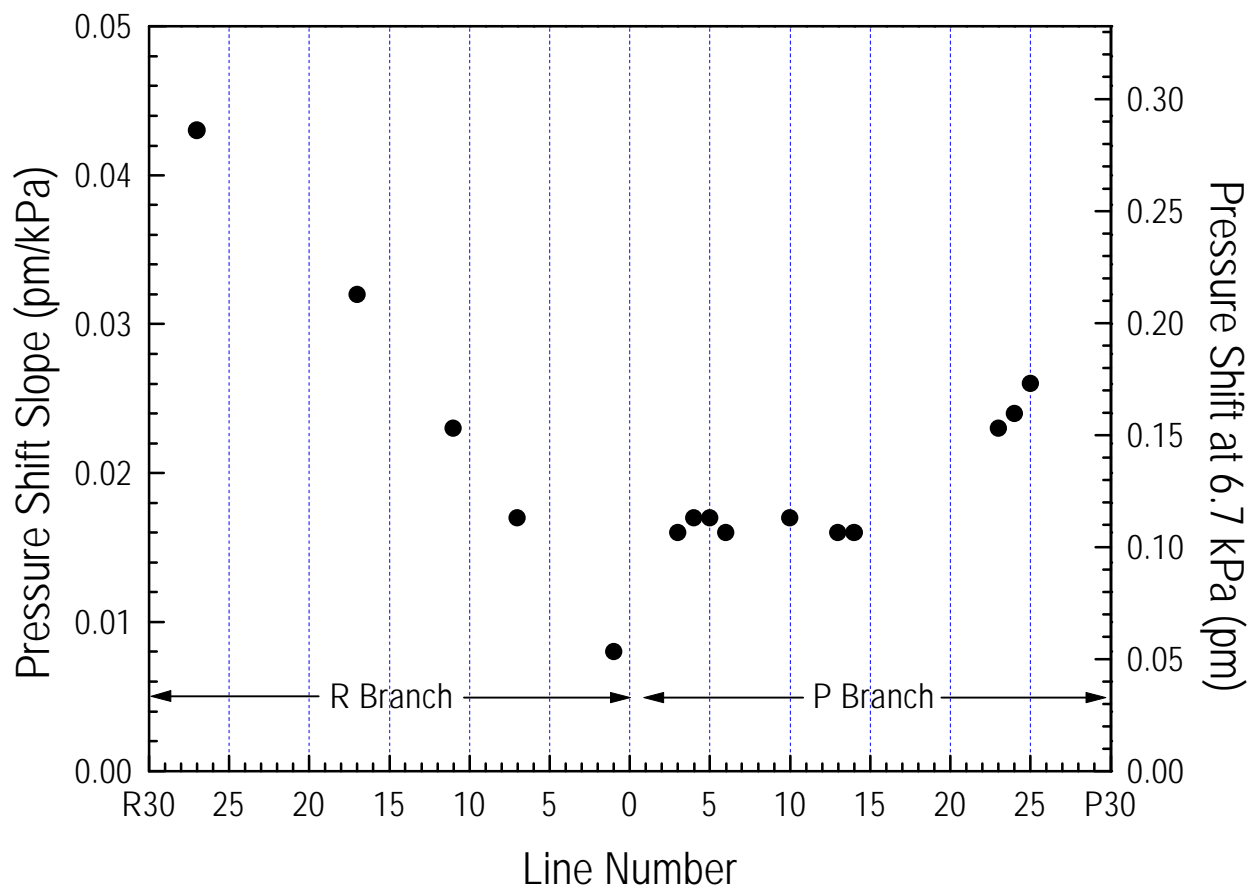


**Figure 2.** Plot of the pressure shift slope and pressure shift at the SRM pressure of 6.7 kPa versus line number for the R and P branches of the  $^{12}\text{C}_2\text{H}_2 \nu_1 + \nu_3$  band. Data are from Ref. 5.

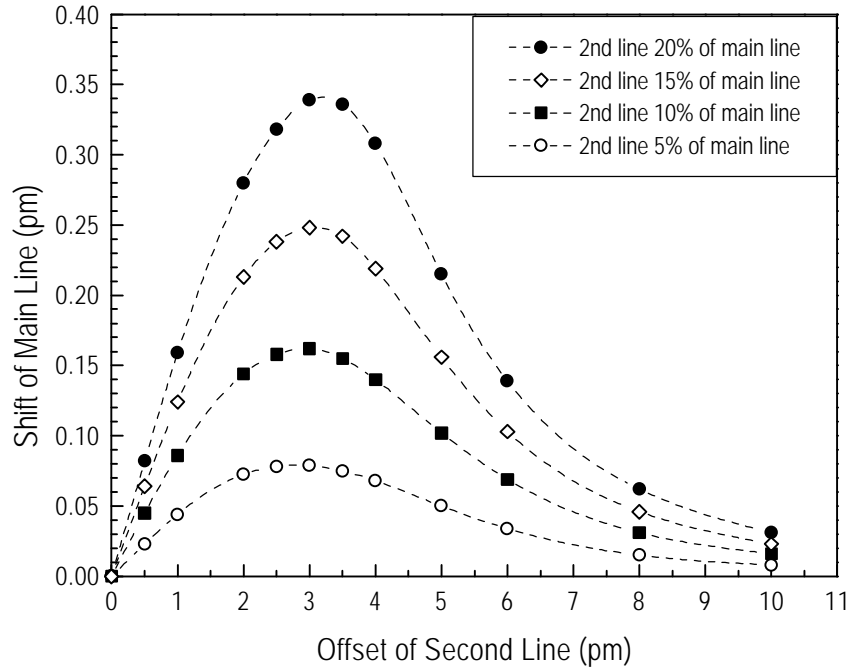


**Figure 3.** Modeling results to determine the effect of nearby lines on the apparent line center of a measured (main) line for the conditions where the nearby (second) line's strength is 5, 10, 15, and 20 % of the main line. The lines were modeled as Lorentzian lines with 5 pm FWHM. The points are the modeling results, and the dashed lines are spline fits to guide the eye.

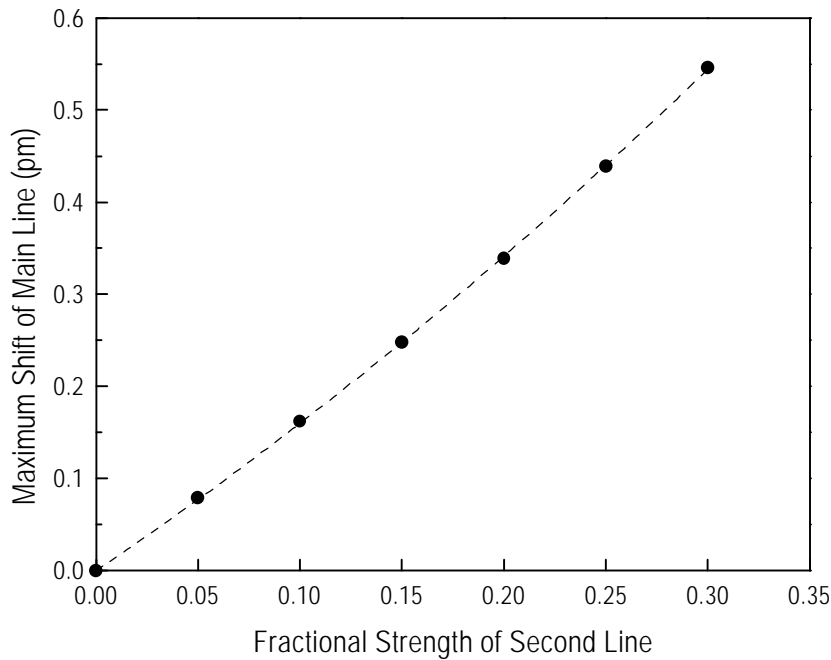


**Figure 4.** Modeling results: plot of the maximum shift of the main line versus fractional strength of the second line. The points are the modeling results. A quadratic fit (dashed line) yields:  $shift (pm) = 1.492 x + 1.076 x^2$ , where  $x$  is the fractional strength of the second line relative to the main line.

## Appendix A

SRM 2517a Certificate

## Appendix B

### Journal Article:

W.C. Swann and S.L. Gilbert, "Pressure-induced shift and broadening of 1510–1540-nm acetylene wavelength calibration lines," *J. Opt. Soc. Am. B* **17**, 1263-1270 (2000).



# National Institute of Standards & Technology

## Certificate

### Standard Reference Material<sup>®</sup> 2517a

High Resolution Wavelength Calibration Reference for 1510 nm – 1540 nm  
Acetylene <sup>12</sup>C<sub>2</sub>H<sub>2</sub>

Serial No.:

This Standard Reference Material (SRM) is intended for wavelength calibration in the spectral region from 1510 nm to 1540 nm. SRM 2517a is a single-mode optical-fiber-coupled absorption cell containing acetylene (<sup>12</sup>C<sub>2</sub>H<sub>2</sub>) gas at a pressure of 6.7 kPa (50 Torr). The absorption path length is 5 cm and the absorption lines are about 7 pm wide. The cell is packaged in a small instrument box (approximately 24 cm long x 12.5 cm wide x 9 cm high) with two FC/PC fiber connectors for the input and output of a user-supplied light source. This SRM can be used for high resolution applications such as calibrating a narrowband tunable laser, or lower resolution applications such as calibrating an optical spectrum analyzer. Acetylene has more than 50 accurately measured absorption lines in the 1500 nm wavelength region.

**Certified Wavelength Values:** The vacuum wavelengths of absorption lines in the R and P branch of the  $\nu_1 + \nu_3$  rotational-vibrational band of <sup>12</sup>C<sub>2</sub>H<sub>2</sub> have been measured previously to high accuracy [1]. These literature values for the vacuum wavelengths were adjusted for the pressure shift due to the collisions between acetylene molecules at the 6.7 kPa (50 Torr) pressure within the SRM cell to obtain the certified wavelength values for this SRM. Details of the measurement procedure and data analysis for the determination of the pressure shift can be found in Reference [2], and the uncertainty analysis for the SRM is documented in Reference [3]. A spectrum of the absorption band is shown in Figure 1 and certified wavelength values are given in Table 1. Figure 2 shows an expanded scan near line P25. The center wavelengths of 15 lines listed in Table 1 are certified with an uncertainty of 0.1 pm, 39 lines are certified with an uncertainty of 0.3 pm, and 2 lines are certified with an uncertainty of 0.6 pm. These uncertainties are the expanded uncertainties using a coverage factor  $k = 2$  (i.e., the quoted uncertainty is  $\pm 2\sigma$ ).

**Expiration of Certification:** The certification of this SRM is indefinite within the measurement uncertainties specified, provided the SRM is handled, stored, and used in accordance with the instructions given in this certificate. The gas is contained in a glass cell with all-glass seals at the windows and the fill port.

Development of the SRM and supporting measurements were performed by S.L. Gilbert and W.C. Swann of the NIST Optoelectronics Division.

Statistical consultation was provided by C.M. Wang of the NIST Statistical Engineering Division.

The support aspects involved in the preparation, certification, and issuance of this SRM were coordinated through the NIST Standard Reference Materials Program by J.W.L. Thomas.

Gordon W. Day, Chief  
Optoelectronics Division

Gaithersburg, MD 20899  
Certificate Issue Date: 11 December 2000

Nancy M. Trahey, Chief  
Standard Reference Materials Program

Table 1. Certified Wavelengths for SRM 2517a

Literature values from Reference [1] are adjusted for the pressure shift due to the 6.7 kPa (50 Torr) cell pressure. These vacuum wavelengths of the  $\nu_1 + \nu_3$  band  $^{12}\text{C}_2\text{H}_2$  are certified with the uncertainty indicated in parenthesis for the last digits. The uncertainties quoted are the expanded uncertainty using a coverage factor  $k = 2$  (i.e., the quoted uncertainty is  $\pm 2\sigma$ ). The lines in bold were accurately characterized by NIST [2] and have the lowest uncertainty.

R Branch	Wavelength (nm)	P Branch	Wavelength (nm)
29	1511.7304(3)	1	1525.7599(6)
28	1512.0884(3)	2	1526.3140(3)
<b>27</b>	<b>1512.45273(12)</b>	<b>3</b>	<b>1526.87435(10)</b>
26	1512.8232(3)	<b>4</b>	<b>1527.44114(10)</b>
25	1513.2000(3)	<b>5</b>	<b>1528.01432(10)</b>
24	1513.5832(3)	<b>6</b>	<b>1528.59390(10)</b>
23	1513.9726(3)	7	1529.1799(3)
22	1514.3683(3)	8	1529.7723(3)
21	1514.7703(3)	9	1530.3711(3)
20	1515.1786(3)	<b>10</b>	<b>1530.97627(10)</b>
19	1515.5932(3)	11	1531.5879(3)
18	1516.0141(3)	12	1532.2060(3)
<b>17</b>	<b>1516.44130(11)</b>	<b>13</b>	<b>1532.83045(10)</b>
16	1516.8747(3)	<b>14</b>	<b>1533.46136(10)</b>
15	1517.3145(3)	15	1534.0987(3)
14	1517.7606(3)	16	1534.7425(3)
13	1518.2131(3)	17	1535.3928(3)
12	1518.6718(3)	18	1536.0495(6)
<b>11</b>	<b>1519.13686(10)</b>	19	1536.7126(3)
10	1519.6083(3)	20	1537.3822(3)
9	1520.0860(3)	21	1538.0583(3)
8	1520.5700(3)	22	1538.7409(3)
<b>7</b>	<b>1521.06040(10)</b>	<b>23</b>	<b>1539.42992(10)</b>
6	1521.5572(3)	<b>24</b>	<b>1540.12544(11)</b>
5	1522.0603(3)	<b>25</b>	<b>1540.82744(11)</b>
4	1522.5697(3)	26	1541.5359(3)
3	1523.0855(3)	27	1542.2508(3)
2	1523.6077(3)		
<b>1</b>	<b>1524.13609(10)</b>		

**Storage and Handling:** The protective caps provided for the FC/PC fiber connectors should be replaced when the SRM is not in use. This SRM is intended to be used in a laboratory environment near ambient room temperature ( $22 \pm 5$ ) °C. The user should avoid exposing the unit to large temperature variations, temperature cycling, or mechanical shock, as these may cause the optical alignment to degrade. Such optical misalignment affects the throughput of the SRM but will not shift the centers of the absorption lines. A more serious but less likely problem is cell breakage or leakage. The unit should be replaced if the linewidths or depths differ significantly from those shown in Figures 1 through 4 when measured using comparable resolution.

**Measurement Conditions and Procedure:** The long term stability of acetylene and the use of fundamental molecular absorption lines render the SRM insensitive to changes in environmental conditions. The purpose of the certification procedure is to verify that the unit contains the correct pressure of  $^{12}\text{C}_2\text{H}_2$  gas and has no significant contaminants that produce additional absorption lines. Measurements are made using a tunable diode laser (~1 MHz linewidth) and a calibrated wavelength meter. Spectra similar to that shown in Figure 2 are taken of each SRM unit and one or more lines are accurately fit to verify the line's center using the procedure described in Reference [2].

## INSTRUCTIONS FOR USE

**General Considerations:** The SRM can be used to calibrate a laser or wavelength measuring instrument in the 1510 nm to 1540 nm region. The values in Table 1 are vacuum wavelengths; if the user requires the wavelength in air, the appropriate correction for the index of refraction of air must be applied (see Reference [4]). Depending on what type of instrument is being calibrated, a user-supplied broadband source or a tunable narrowband source may be used. Typical optical connections are shown in Figure 5. The unit is bi-directional (has no preferred input/output port); connections to the unit should be made using single-mode optical fibers terminated with clean FC/PC connectors.

**Use With a Broadband Source:** A broadband source in the 1500 nm region (such as a light emitting diode, white light, or amplified spontaneous emission source) is useful when calibrating an instrument such as a diffraction grating-based optical spectrum analyzer. A schematic for this type of calibration is shown in Figure 5(a). Light from the broadband source is coupled into the SRM and the output (transmission through the SRM) is connected to the instrument that is being calibrated. The absorption lines of acetylene appear as dips in the spectrum of the light source. In general, the dips will not be as deep as those shown in Figure 1; most instruments of this type will have a resolution bandwidth that is significantly larger than the widths of the SRM absorption lines. An example of this effect is shown in Figures 3 and 4, where the spectrum in the region of lines P8–10 is observed using a tunable diode laser (Figure 3) or a broadband source and an optical spectrum analyzer set to 0.05 nm resolution (Figure 4).

**Use With a Tunable Source:** The SRM can be used to calibrate the wavelength scale of a tunable source in this region (such as a diode laser, a fiber laser, or a source filtered by a tunable filter). A schematic for this type of calibration is shown in Figure 5(b). The laser is tuned over one or more of the acetylene absorption lines. The transmission through the SRM is monitored by a detector; the transmitted power passes through a minimum at the center of an absorption line. Alternatively, a tunable laser source and the SRM can be used to check the calibration of a wavelength meter by measuring the wavelength of the laser (using the wavelength meter) as the laser is tuned through an absorption line.

**Suggested Procedure for Low-Accuracy Requirements; Calibration Uncertainty > 30 pm:** If calibrating an instrument using a broadband source, use an instrument resolution of  $\leq 0.1$  nm. If using a tunable source, use a data point density of at least one point every 0.005 nm (5 pm). After identifying a particular absorption line by comparing to the spectrum in Figure 1, find the center or minimum point of the line. Calibrate the instrument to the center wavelength of this line (from Table 1) using the calibration procedure specified by the instrument manufacturer. The instrument's linearity can be checked by repeating the procedure for a different absorption line and comparing it to the value listed in Table 1.

**Suggested Procedure for Moderate-Accuracy Requirements; Calibration Uncertainty in the Approximate Range of 3 pm to 30 pm:** If the source power varies significantly with wavelength, divide the SRM transmission spectrum by the source spectrum to obtain a normalized trace. After identifying a particular absorption line by comparing to the spectrum in Figure 1, make a high resolution scan of the line. If calibrating an instrument using a broadband source, use an instrument resolution of  $\leq 0.05$  nm. If using a tunable source, use a data point density of at least one point every 0.002 nm (2 pm). Find the wavelength readings on both sides of the line where the absorption is 50 % of the maximum; the line center is half-way between these two wavelength readings. For higher accuracy results, repeat this procedure five times and take the average of the measurements. Alternatively, the line center can be determined by fitting the central portion using a 4th order polynomial. Calibrate the instrument to the center wavelength of this line (from Table 1) using the calibration procedure specified by the instrument manufacturer. The

instrument's linearity can be checked by repeating the procedure for a different absorption line and comparing it to the value listed in Table 1.

**Suggested Procedure for High-Accuracy Requirements; Calibration Uncertainty < 3 pm:** Connect a narrowband tunable light source (source bandwidth  $\leq 1$  pm) to one of the fiber connectors on the SRM unit. After identifying a particular absorption line by comparing to the spectrum in Figure 1, make a high resolution scan of the line. Use a data point density of at least one point every 1 pm and divide the SRM transmission spectrum by the source spectrum to obtain a normalized trace. Using a fitting technique such as the least squares, fit the absorption data to a Lorentzian or Voigt lineshape. Details of a line fitting procedure and potential errors sources can be found in Reference [2], which is also included as an appendix in Reference [3]. Calibrate the instrument to the center wavelength of this line (from Table 1) using the calibration procedure specified by the instrument manufacturer. The instrument's linearity can be checked by repeating the procedure for a different absorption line and comparing it to the value listed in Table 1. **NOTE:** Highly reproducible *relative* wavelength measurements can be made using the procedure described for moderate-accuracy requirements. However, due to the presence of nearby lines, the procedure described in this paragraph is recommended to achieve high-accuracy *absolute* wavelength calibration.

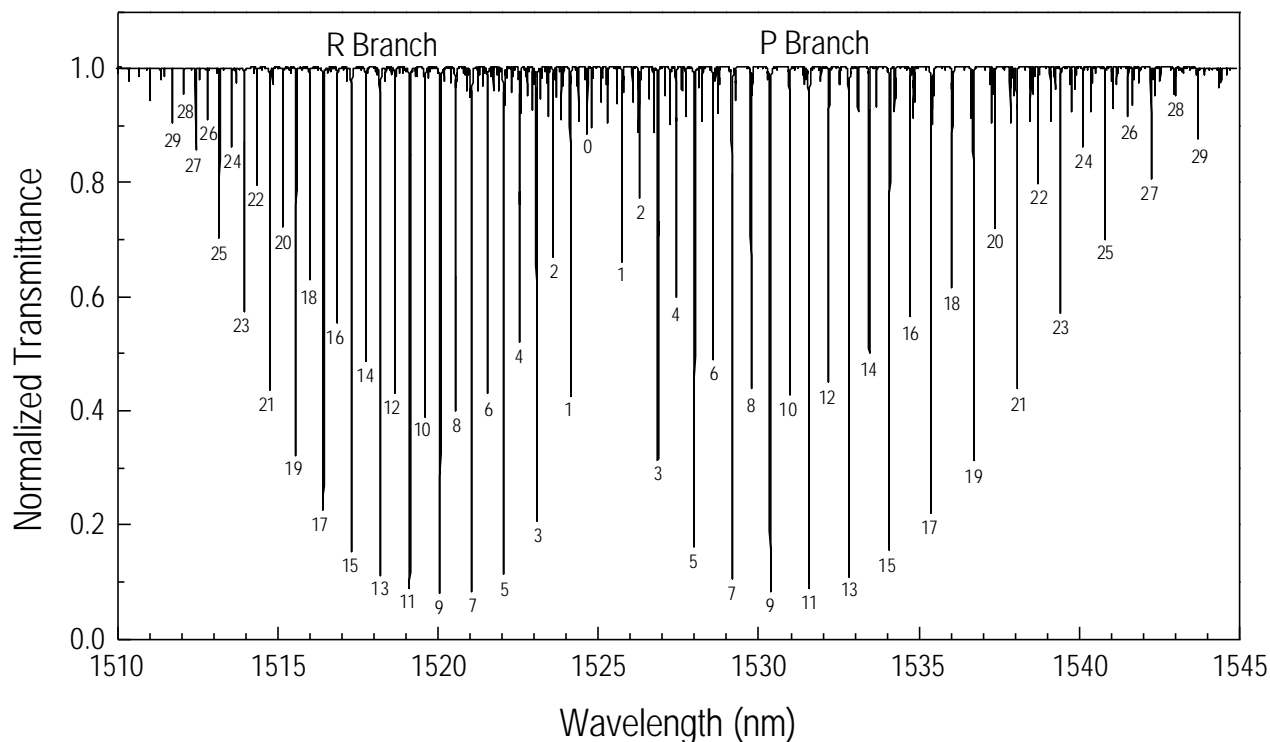


Figure 1. Normalized spectrum of SRM 2517a obtained by scanning a tunable diode laser and measuring the laser power transmitted through a SRM unit. The SRM contains a 5 cm long absorption cell filled with acetylene  $^{12}\text{C}_2\text{H}_2$  to a pressure of 6.7 kPa (50 Torr). A file containing these data can be downloaded from NIST at <http://ois.nist.gov/srmcatalog/datafiles/>.

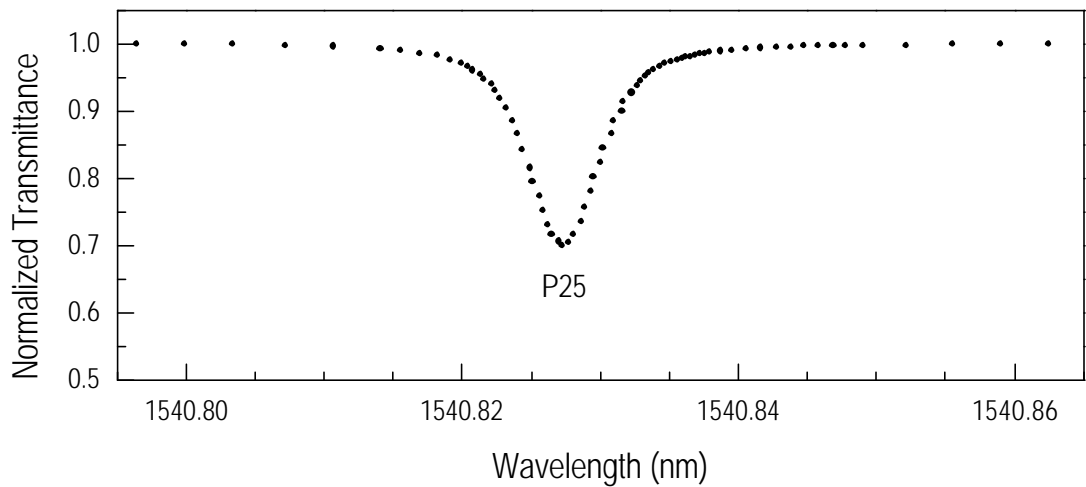


Figure 2. Spectrum of line P25 from Figure 1 obtained by scanning a tunable diode laser

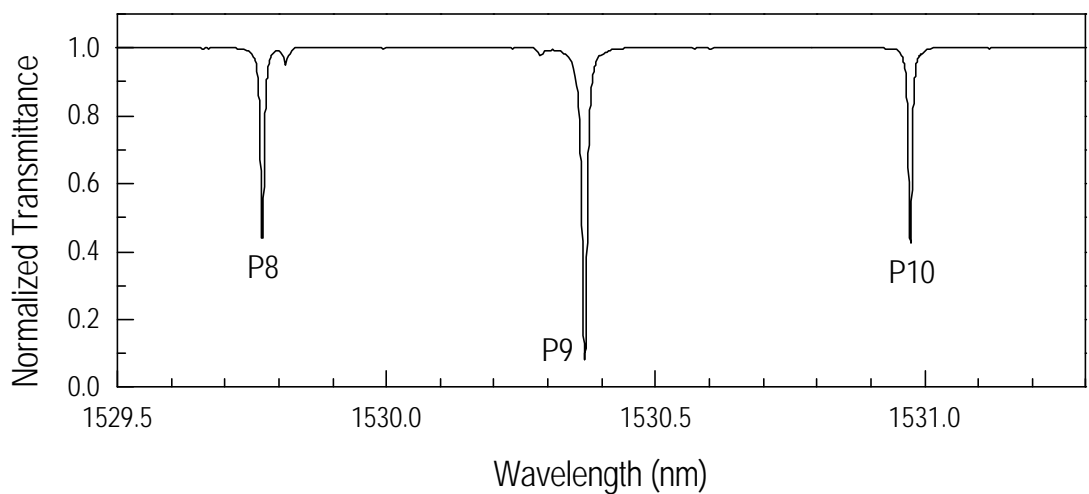


Figure 3. Spectrum of the P8, P9, and P10 lines from Figure 1 obtained by scanning a tunable diode laser

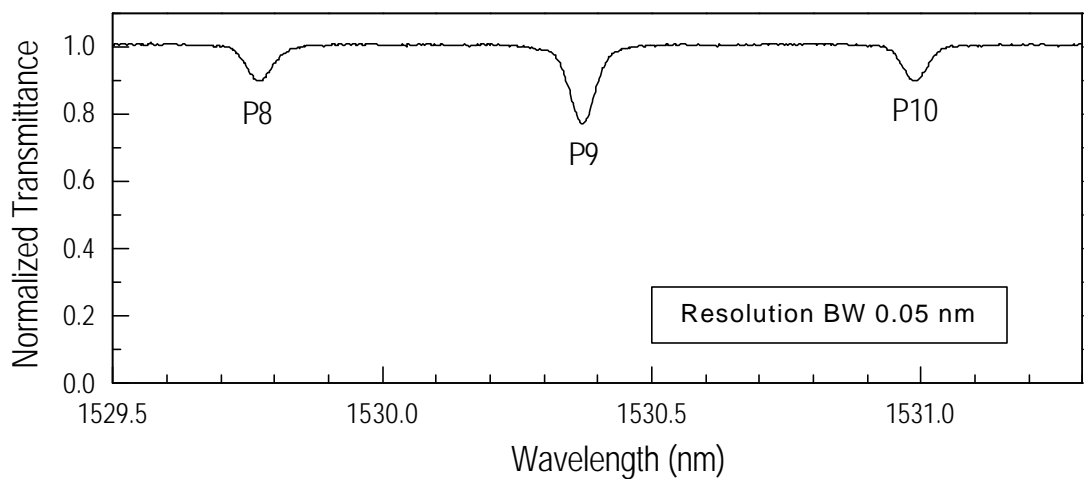
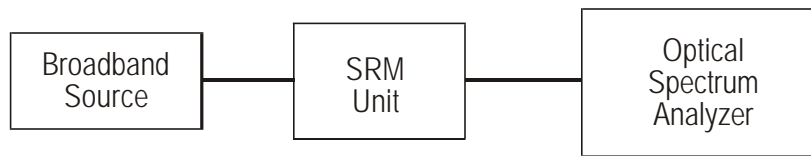


Figure 4. Spectrum of the P8, P9, and P10 lines obtained using a broadband source and an optical spectrum analyzer set to 0.05 nm resolution



(a)



(b)

Figure 5. (a) Schematic of technique when using the SRM and a broadband source to calibrate an optical spectrum analyzer. (b) Schematic of technique when using the SRM to calibrate a tunable source. A wavelength meter can be calibrated by using a tunable laser in the configuration shown in (b) and measuring its wavelength using the wavelength meter.

#### REFERENCES

- [1] Nakagawa, K., Labachellerie, M., Awaji, Y., and Kouroggi, M., "Accurate Optical Frequency Atlas of the 1.5  $\mu\text{m}$  Bands of Acetylene," *J. Opt. Soc. Am. B* **13**, pp. 2708-2714, (1996).
- [2] Swann, W.C. and Gilbert, S.L., "Pressure-Induced Shift and Broadening of 1510 to 1540 nm Acetylene Wavelength Calibration Lines," *J. Opt. Soc. Am. B*, **17**, pp. 1263-1270, (2000).
- [3] Gilbert, S.L. and Swann, W.C., "Acetylene  $^{12}\text{C}_2\text{H}_2$  Absorption Reference for 1510 to 1540 nm Wavelength Calibration – SRM 2517a," NIST Special Publication 260-133 (revised 2000), In Press.
- [4] Edlen, B., "The Refractive Index of Air," *Metrologia*, **2**, p. 12, (1966); and *CRC Handbook of Chemistry and Physics*, 77th Ed., pp. 10-266, (1996).

*Users of this SRM should ensure that the certificate in their possession is current. This can be accomplished by contacting the SRM Program at: telephone (301) 975-6776; fax (301) 926-4751; e-mail [srminfo@nist.gov](mailto:srminfo@nist.gov); or via the Internet <http://www.nist.gov/srm>.*

# Pressure-induced shift and broadening of 1510–1540-nm acetylene wavelength calibration lines

W. C. Swann and S. L. Gilbert

*Division of Optoelectronics, Electronics and Electrical Engineering Laboratory, National Institute of Standards and Technology, Boulder, Colorado 80303*

Received November 1, 1999; revised manuscript received January 24, 2000

We have measured the pressure-induced shift for 15 lines of the  $\nu_1 + \nu_3$  rotational–vibrational band of acetylene  $^{12}\text{C}_2\text{H}_2$ . These lines are useful as wavelength references in the 1510–1540-nm region. We find that the pressure shift varies from +0.008(2) pm/kPa for line *R*1 to +0.043(2) pm/kPa for line *R*27, with many of the lines exhibiting a shift near +0.017 pm/kPa (or, equivalently,  $+2.3 \times 10^{-3}$  pm/Torr or  $-0.29$  MHz/Torr). In addition, we have measured the pressure broadening of these lines and find that it also varies with line number and is typically  $\sim 0.7$  pm/kPa ( $\sim 12$  MHz/Torr). We also evaluate the line sensitivity to temperature changes and electromagnetic fields. [S0740-3224(00)01007-9]

*OCIS codes:* 020.3690, 060.2330, 120.3940, 120.4800, 300.6260, 300.6390, 300.0300.

## 1. INTRODUCTION

Wavelength references are important in the 1500-nm region to support wavelength-division-multiplexed optical fiber communication systems. In a wavelength-division-multiplexed system many wavelength channels are sent down the same fiber, thereby increasing the bandwidth of the system by the number of channels. If one channel's wavelength were to shift, cross talk could occur between that channel and a neighboring channel. To calibrate instruments that are used to characterize components and monitor the wavelengths of the channels, wavelength references are needed.

Fundamental atomic or molecular absorptions provide wavelength references that are stable under changing environmental conditions such as temperature and pressure variations or the presence of electromagnetic fields. There are several good molecular transitions in the 1500-nm region. The acetylene  $^{12}\text{C}_2\text{H}_2$   $\nu_1 + \nu_3$  rotational–vibrational combination band, shown in Fig. 1, contains  $\sim 50$  strong lines between 1510 and 1540 nm. The corresponding band in  $^{13}\text{C}_2\text{H}_2$  extends from  $\sim 1520$  to  $\sim 1550$  nm. Hydrogen cyanide also has a good spectrum, with lines between 1530 and 1565 nm for  $\text{H}^{13}\text{C}^{14}\text{N}$ . The National Institute of Standards and Technology (NIST) has developed wavelength calibration transfer standards based on acetylene and hydrogen cyanide.<sup>1,2</sup>

The vacuum wavelengths of the acetylene  $\nu_1 + \nu_3$  lines have been measured at low pressure with an uncertainty of  $\sim 10^{-6}$  nm.<sup>3</sup> For a wavelength reference, the stability of the wavelength of each absorption line is a critical characteristic. The symmetric isotopic species of acetylene are particularly insensitive to external perturbation because they have no permanent dipole moment. The largest potential source of line shift is energy-level shift caused by the interaction of the molecules during elastic collisions.<sup>4</sup> Commonly called the pressure shift, this

shift depends linearly on the collision frequency. An upper limit for the pressure shift of 200 kHz/Torr (1.5 kHz/Pa) has been reported for one acetylene line at low pressure.<sup>5</sup> For wavelength calibration of instruments, however, it is often desirable to use an intermediate- or high-pressure sample to match the reference bandwidth to the instrument resolution. This results in the strongest signals for a given resolution bandwidth.

We have measured the pressure-induced shift and broadening for 15 lines in the  $\nu_1 + \nu_3$  rotational–vibrational band of acetylene  $^{12}\text{C}_2\text{H}_2$ . We describe our measurement procedure in Section 2 and summarize the results in Section 3. In Section 4 we estimate the line center sensitivity to temperature changes and electromagnetic fields. Conclusions are given in Section 5.

## 2. MEASUREMENT DESCRIPTION AND DATA ANALYSIS

A schematic diagram of our pressure shift measurement apparatus is shown in Fig. 2. Light from a tunable diode laser is sent through two absorption cells simultaneously, and the transmission through each cell is monitored by detectors. One cell contains acetylene gas at low pressure, and the other contains either intermediate or high pressure, as specified below. A third detector monitors the laser power, and a wavelength meter measures the laser's wavelength with an uncertainty of 1 part in  $10^7$  (0.15 pm at 1500 nm). A computer controls the laser wavelength scan and records the readings of the three detectors and wavelength meter.

Three absorption cells were filled with acetylene  $^{12}\text{C}_2\text{H}_2$  at low pressure ( $6.7 \pm 0.1$  kPa,  $\sim 50$  Torr), intermediate pressure ( $29.7 \pm 0.5$  kPa,  $\sim 225$  Torr), and high pressure ( $66 \pm 1$  kPa,  $\sim 500$  Torr). The pressure uncertainty quoted here is the expanded uncertainty obtained with a

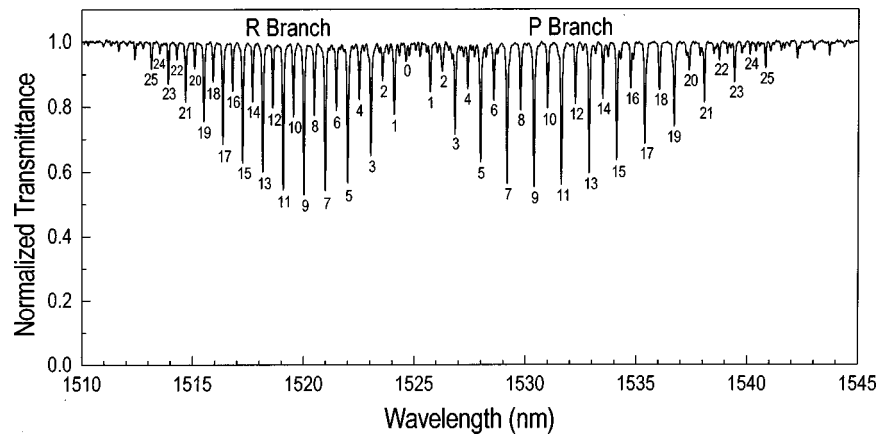


Fig. 1. Acetylene ( $^{12}\text{C}_2\text{H}_2$ ) spectrum taken by passing LED light through a 5-cm-long absorption cell and recording the spectrum of the transmitted light with an optical spectrum analyzer with 0.05-nm resolution. This spectrum has been normalized to the LED spectrum.

coverage factor  $k = 2$  (i.e., our quoted uncertainty is  $\pm 2\sigma$ ).<sup>6</sup> The fused-silica absorption cells are 5 cm long, with windows fused to the cells by a glass frit method. To prevent interference fringes in the transmitted signal the windows are mounted at an angle of  $11^\circ$  and are also wedged by  $\sim 2^\circ$ . The cells were first evacuated and leak checked and were then filled with isotopically pure gas (99.96%  $^{12}\text{C}_2\text{H}_2$ ). During the fill process the pressure in the fill manifold (and hence the cell) was monitored with a capacitance manometer and a strain gauge pressure sensor. Once filled, the cells were closed off with a glass valve with o-ring seals.

Figure 3 shows spectra of line  $P_4$  obtained with the low- and the high-pressure cells. The pressure broadening in the high-pressure spectrum is obvious. We are primarily interested in the shift of the high-pressure line relative to the low-pressure line. Fifteen lines were scanned by this technique, and 13 of these lines were also scanned by use of the low- and the intermediate-pressure cells. The measured quantity, the transmitted power  $I_T$ , is related to the absorption coefficient  $\alpha$  and the absorption path length  $L$  by

$$I_T = I_0 \exp(-\alpha L), \quad (1)$$

where  $I_0$  is the incident power. We first divided the cell transmission curves by the laser power monitor signal to remove common-mode intensity variations and normalized the data. We then took the natural logarithm to obtain the absorbance  $\alpha L$ .

Individual lines were then fitted to Voigt profiles<sup>4</sup> by use of an orthogonal distance regression algorithm.<sup>7</sup> The orthogonal distance regression, called either error-in-variables or total-least-squares regression, obtains the model parameters by minimizing the sum of squares (SS) of the orthogonal distances from the model to the data points. The fitting program was able to account for a background slope and uncertainties in both  $x$  (wavelength) and  $y$  (transmitted power). A Voigt profile is a convolution of Lorentzian and Gaussian profiles; it results when there is a combination of Gaussian broadening (resulting from Doppler broadening, for example) and Lorentzian line shape (resulting from the natural linewidth or pressure broadening, for example). In our situation the natural linewidth is small compared with the

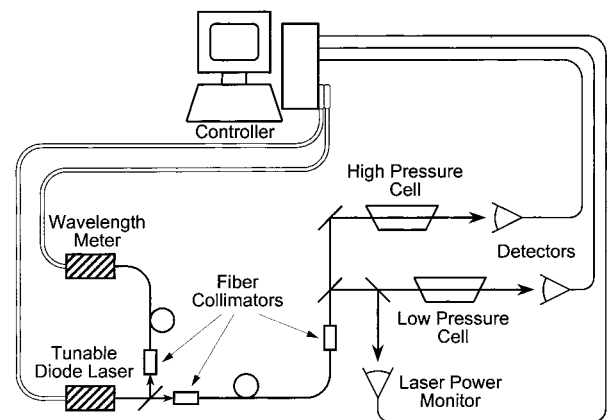


Fig. 2. Diagram of pressure shift measurement apparatus.

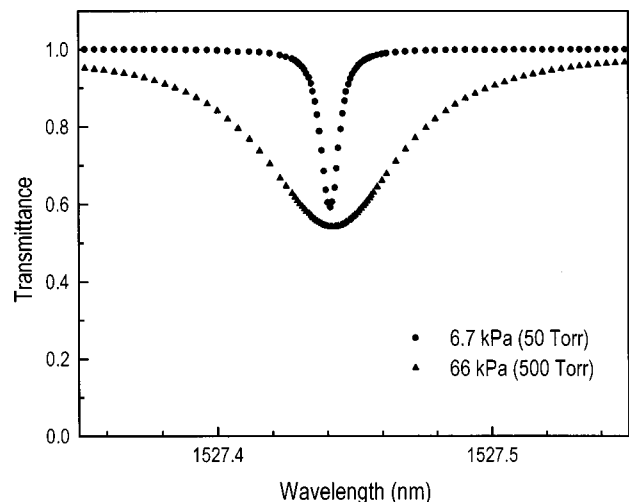


Fig. 3. Tunable diode laser scan of the  $^{12}\text{C}_2\text{H}_2$  line  $P_4$  showing the transmittance through the low- and the high-pressure cells.

Gaussian Doppler broadening and the Lorentzian pressure broadening. For the low-pressure data, the width of the Lorentzian component and the width of the Gaussian component are comparable. For the intermediate- and the high-pressure data, the Lorentzian component dominates because of the larger pressure broadening. For the

line fitting, we fixed the Gaussian Doppler linewidth at 3.7 pm (Ref. 4) and allowed other model parameters to vary.

Since the spectra for the low- and the high-pressure cells were measured simultaneously, the absolute accuracy of the wavelength meter was not of critical importance for the relative pressure shift measurement. However, the short-term statistical variation of the wavelength measurement did add noise to the data. To determine this statistical variation we took repeated measurements of a laser stabilized to a narrow rubidium line. The statistical variation of repeated measurements yielded a Gaussian distribution with a standard deviation of 0.1 pm. We determined the experimental uncertainty in transmitted power by measuring the statistical variation of the data within a region of the line wing. The standard deviation of these fluctuations was 1 part in  $10^4$  of the transmitted power.

Each data point was assigned a standard uncertainty of 0.1 pm for the wavelength and a fractional uncertainty of 1 part in  $10^4$  for the transmitted power. The fitting program determined the line centers and their widths, the corresponding uncertainties, and the reduced residual-SS ( $\chi^2$ ) value for the fit. Several factors can complicate the fitting procedure and can cause uncertainty in the line center measurement. Our approaches to minimizing and measuring the effect of these contributions are discussed below.

#### A. Background Signal Variation

A slope or a variation in the background level can shift the apparent center of a line, particularly for the wide lines of the intermediate- and the high-pressure cells. Interference fringes due to reflected laser light, wavelength dependence of the optical components, beam pointing stability, and variations in the laser power can cause background variation. As mentioned above, we removed common-mode laser power variations by dividing the cell transmittance data by the power monitor data. Owing to the wavelength dependence of optical fiber couplers (splitters), we used free-space beam splitters to send the laser light to the cells and the power monitor. We minimized interference effects by using wedged cell windows and beam splitters, windowless detectors, and two optical isolators. These measures reduced the statistical power fluctuations to 1 part in  $10^4$  and the residual slope to less than 5 parts in  $10^4$  over a 250-pm scan. This residual slope was  $\sim 1$  order of magnitude less than that caused by small spectra features discussed below and is consequently insignificant compared with spectral effects.

#### B. Overlap with Nearby Lines

Wings of nearby lines can skew the shape of the line being measured and can shift its apparent center. In addition to the strong lines of the  $\nu_1 + \nu_3$  band, there are a number of weak lines throughout the spectrum that are due to hot bands (transitions that are not out of the ground vibrational state).<sup>8</sup> Figure 4 is a plot of the absorbance between 1526 and 1529 nm, showing lines *P2*–*P6* of the  $\nu_1 + \nu_3$  band and weaker hot band lines. To minimize the effect of neighboring lines on our pressure shift measurement we deliberately avoided measuring lines in the

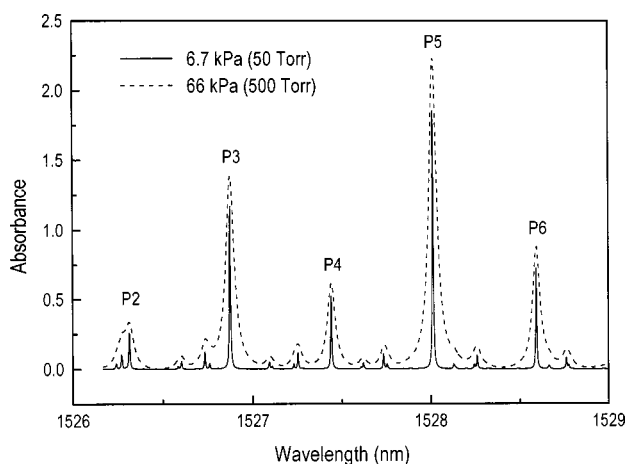


Fig. 4. Plot of  $^{12}\text{C}_2\text{H}_2$  absorbance  $\alpha L$  between 1526 and 1529 nm for the low- and the high-pressure cells.

spectrum that have significant lines very close to the primary line (such as line *P2*). We used high-resolution spectra<sup>8</sup> to select lines that were relatively isolated from other lines. This eliminated the large perturbations, but some smaller lines were present in the vicinity of several measured primary lines.

The apparent shift due to smaller lines is most significant for the broader high-pressure lines, where small lines can be buried within the primary line. We estimated the effect of these lines by modeling the worst cases. The high-pressure data were modeled with Lorentzian line shapes that approximate the spectra in the vicinity of lines *R1*, *P4*, and *P14*. These primary lines had small lines located  $\sim 35$  pm from their line centers. The line parameters were obtained from the low-pressure data, with the linewidths scaled up to account for pressure broadening. White noise was added to the pure Lorentzian shapes to simulate real data. We initially limited the line fitting to the central portion of the line within 85% of the maximum absorbance. Adding small lines, modeled as described above, resulted in a shift in the line center value returned by the fitting program for the (modeled) primary line. We found that the fitted line center of the primary line is most sensitive to additional lines that are very near the line center. Even a very small line (absorbance  $\approx 1\%$  of the primary line) can cause an apparent line shift of  $\sim 0.2$  pm if it is within 50 pm of the center of the primary line. In our modeling of the three primary lines the apparent shift due to small neighboring lines was as much as 0.4 pm, and the reduced  $\chi^2$  value was as large as 6. Restricting the fit range to the central portion of the line, within 65% of the maximum absorbance, reduced the  $\chi^2$  values to  $\sim 1$ , indicating a good fit, and restored the original (unperturbed) line center. Restricting the fit range further did not significantly effect the results.

We compared the modeling results with those obtained from the measured data and observed similar trends. For the high-pressure data, primary lines with nearby weak lines gave relatively poor fits ( $\chi^2$  between 1.6 and 3.4) when fitted over 85% of the maximum absorbance. Narrowing the fit range to within 65% of maximum absorbance reduced the  $\chi^2$  values to  $\sim 1$  and changed the fit-

ted line center by as much as 0.2 pm; further narrowing of the fit range had a negligible effect.

The combination of avoiding primary lines with significant nearby lines and reducing the fit range to within 65% of the maximum absorbance eliminates the line-overlap skewing effect for most cases. To first order, the small line wings could be approximated by a slope in the background when the fit was restricted to a narrow region around the line center. The fitting program was able to remove this effect by removing a slope in the region of the main line. If the fit range was too wide, however, the simple slope approximation was not adequate. Since we cannot be certain that there are no small lines closer than 35 pm from a primary line center, we assign a standard uncertainty (estimated standard deviation) for each of the relative line centers: of 0.07 pm for the high-pressure data and 0.04 pm for the intermediate-pressure data, owing to residual effects of additional lines. These uncer-

tainty estimates are derived from the variation of the line centers as we changed the width of the fitting region. In view of the good  $\chi^2$  values obtained, we believe that this uncertainty estimate is conservative.

### C. Line Fitting Reproducibility

To test the reproducibility of the line fit we took several scans of the same lines and determined the pressure shift for each scan. Since the wavelength meter could drift slightly between each scan, we compared only the shift measurement, not the individual line center measurements. From these measurements we estimate that the standard deviation for the line shift is 0.03 pm. Since this is an uncertainty in the shift measurement and not an uncertainty in the individual line centers, we then divide this value by  $\sqrt{2}$  and assign a standard uncertainty of 0.02 pm for both the low-pressure and the higher-pressure cell data.

**Table 1. Uncertainty Budget<sup>a</sup>**

Source of Uncertainty	Relative Line Center Standard Uncertainty (pm)		
	Low-Pressure Cell (6.7 kPa)	Intermediate-Pressure Cell (29.7 kPa)	High-Pressure Cell (66 kPa)
Nearby line contribution	–	0.04	0.07
Fit statistical uncertainty	0.02	0.02	0.02
Fit reproducibility	0.02	0.02	0.02
Combined standard uncertainty	$u_c(\text{low}) = 0.03$	$u_c(\text{int}) = 0.05$	$u_c(\text{high}) = 0.08$

<sup>a</sup>This uncertainty budget was used for the determination of relative line centers for the low-, intermediate-, and high-pressure cells. The combined standard uncertainties are the root SS of the standard uncertainties due to the sources listed. The absolute accuracy of the wavelength meter is not included.

**Table 2. Pressure Shift Results<sup>a</sup>**

Line	Intermediate – Low Pressure $\Delta P = 23.0 \pm 0.6$ kPa		High – Low Pressure $\Delta P = 59.3 \pm 1.3$ kPa		Weighted Average	
	Shift (pm)	Shift Slope (pm/kPa)	Shift (pm)	Shift Slope (pm/kPa)	Shift Slope (pm/kPa)	Shift Slope (MHz/Torr)
R27	0.99(12)	0.043(5)	2.56(17)	0.043(3)	0.043(2)	–0.73(3)
R17	0.72	0.031	1.89	0.032	0.032(2)	–0.55(3)
R11	0.53	0.023	1.39	0.023	0.023(2)	–0.39(3)
R7	0.39	0.017	1.02	0.017	0.017(2)	–0.29(3)
R1	0.15	0.007	0.46	0.008	0.008(2)	–0.14(3)
P3	0.37	0.016	0.98	0.017	0.016(2)	–0.27(3)
P4	0.42	0.018	1.02	0.017	0.017(2)	–0.29(3)
P5	0.40	0.017	1.01	0.017	0.017(2)	–0.29(3)
P6	–	–	0.96	0.016	0.016(3)	–0.27(5)
P10	0.35	0.015	1.02	0.017	0.017(2)	–0.29(3)
P13	0.35	0.015	0.98	0.017	0.016(2)	–0.27(3)
P14	0.37	0.016	0.98	0.017	0.016(2)	–0.27(3)
P23	0.50	0.022	1.36	0.023	0.023(2)	–0.39(3)
P24	–	–	1.44	0.024	0.024(3)	–0.41(5)
P25	0.58	0.025	1.53	0.026	0.026(2)	–0.44(3)

<sup>a</sup>Pressure shift results obtained from the two cell pairs for the measured lines of the  $\nu_1 + \nu_3$  band of acetylene  $^{12}\text{C}_2\text{H}_2$  are shown. The uncertainties in the final digits of the values are indicated in parentheses. For the data in columns 2–5, all the values in a particular column have the uncertainty listed for the first value in the column. The uncertainties quoted are the expanded uncertainties obtained by use of a coverage factor  $k = 2$  (i.e., our quoted uncertainty is  $\pm 2\sigma$ ).

#### D. Wavelength Accuracy

Although the absolute accuracy of the wavelength measurement was not relevant to the pressure shift measurement, extrapolating our line center measurements to zero pressure and comparing with literature values serves as a good verification of our measurements. To determine the line center accuracy for our measurements we first checked the accuracy of the wavelength meter used in the measurements. We have set up a high-accuracy wavelength reference for this purpose.<sup>2</sup> Diode laser light at 1560.5 nm is amplified with an erbium-doped fiber amplifier and is frequency doubled in a periodically poled lithium niobate crystal. The resultant 780-nm light is then used to conduct saturated absorption spectroscopy on the  $5S_{1/2} \rightarrow 5P_{3/2}$  transitions of rubidium ( $^{85}\text{Rb}$  and  $^{87}\text{Rb}$ ). The line centers of the hyperfine components of these transitions have been measured with an uncertainty of  $\pm 0.4$  MHz (Ref. 9); a subset of these lines has been measured to higher accuracy.<sup>10</sup> We stabilized the laser to several different hyperfine components of the  $^{87}\text{Rb}$  transition and compared the wavelength meter reading (vacuum wavelength) to the literature values multiplied by 2. Since the lines were very narrow (less than 10 MHz), the absolute stability of the laser was much better than the quoted wavelength meter uncertainty of 1 part in  $10^7$  ( $\sim 20$  MHz at 1560 nm). From measurements taken before and after our pressure shift scans we found that the wavelength meter reading was offset by  $-0.20 \pm 0.06$  pm ( $+25 \pm 8$  MHz). The uncertainty ( $2\sigma$ ) is derived from the standard deviation of 10 measurements made over a six-month period. During this time the wavelength meter offset varied from  $-0.16$  to  $-0.23$  pm.

### 3. PRESSURE SHIFT, LINE CENTER, AND PRESSURE BROADENING RESULTS

The uncertainty budget for the relative line center determinations is given in Table 1. Table 2 summarizes the line-shift measurement results for the low-intermediate-pressure pair and the low-high-pressure pair. We determined a weighted average slope for the pressure shift for each line. In all cases the wavelength shift was positive with increasing pressure. Figures 5(a) and 5(b) are plots of line center versus pressure for the measured lines of the *R* and the *P* branches, respectively. As expected, each line's shift is consistent with a linear dependence on pressure. For most of the lines in the *P* branch, the shift was approximately  $+0.017$  pm/kPa (or, equivalently,  $+2.3 \times 10^{-3}$  pm/Torr or  $-0.29$  MHz/Torr). The *R* branch exhibited more variation in the pressure shift, with an approximately linear dependence on line number. For both branches, the pressure shift was considerably larger for lines far from the band center (i.e., transitions between states with high rotational quantum numbers), rising to  $+0.043$  pm/kPa for line *R27*.

Using the line center data adjusted for the wavelength meter offset discussed in Subsection 2.D, we extrapolated the line centers to zero pressure, using linear regression fitting. Table 3 summarizes our determinations of the line centers and compares them to the more accurate measurements reported in Ref. 3, which were measured

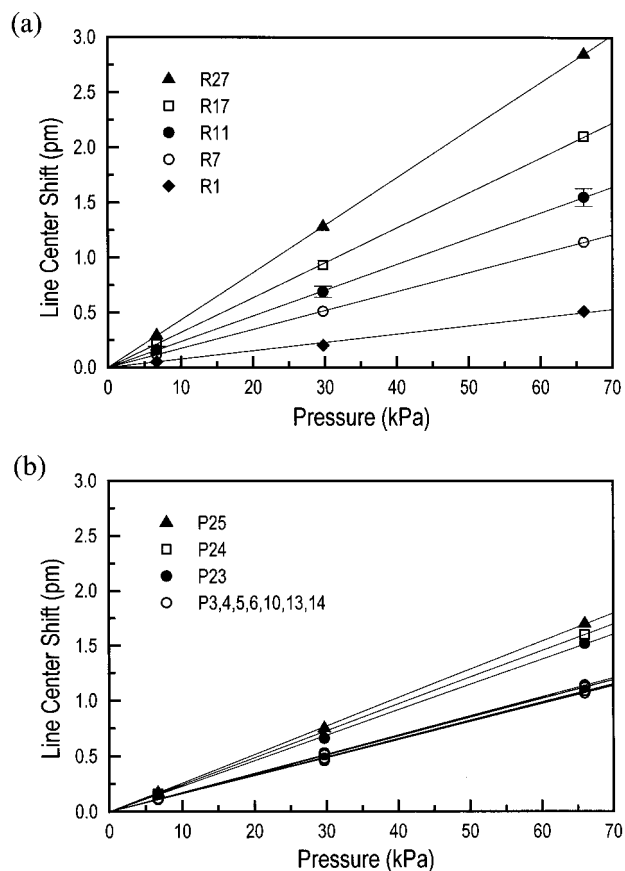


Fig. 5. (a) Pressure shift of the line centers for the measured lines in the  $^{12}\text{C}_2\text{H}_2$  *R* branch. Each line is shown with a linear least-squares fit to the data. (b) Pressure shift of the line centers for the measured lines in the  $^{12}\text{C}_2\text{H}_2$  *P* branch, with corresponding linear least-squares fits. The uncertainties for the other data shown in (a) and (b) are the same as those shown for *R11*.

at 1–4 Pa (10–30 mTorr). Our expanded uncertainty is 0.1 pm (coverage factor of 2), which is twice the root SS of the relative line center standard uncertainty (0.03 pm), the wavelength meter calibration standard uncertainty (0.03 pm), and the linear regression fit uncertainty (0.03 pm). The estimated uncertainty given in Ref. 3 is  $1.2 \times 10^{-6}$  nm. All our line center values are in good agreement with those of Ref. 3; the differences between our measurements and those reported in Ref. 3 are within our uncertainty for each line center. This gives us further confidence in our analysis of the line center values.

Pressure broadening is responsible for the Lorentzian component of the Voigt line shape. We found that the pressure broadening also varied with line number. In contrast to the pressure shift dependence, however, the pressure broadening was largest for lines near the band center (transitions between states with low rotational quantum numbers). Table 4 summarizes our results for the width of the Lorentzian component of the Voigt line shape, where the Gaussian component (which is due to Doppler broadening at room temperature) was fixed at 3.7 pm. The width variation with line number can be seen more clearly in Fig. 6, where we plot the Lorentzian component of the linewidth for the lines measured in the *R* branch and the associated linear fit results. The Lorent-

zian linewidth slope versus pressure, derived from these least-squares fits, is also given in Table 4. Our uncertainty for the Lorentzian linewidth values was derived from the variation that we observed when using different fitting algorithms for the Voigt profile. Although the fitting algorithms agreed for the line centers, values for the Lorentzian component of the linewidth differed slightly.

**Table 3. Unperturbed Line Center Values<sup>a</sup>**

Line	Line Center This Measurement (nm)	Line Center from Ref. 3 (nm)	Difference (pm)
R27	1512.45242	1512.45244	-0.02
R17	1516.44113	1516.44109	0.04
R11	1519.13678	1519.13671	0.07
R7	1521.06034	1521.06029	0.05
R1	1524.13602	1524.13604	-0.02
P3	1526.87430	1526.87424	0.06
P4	1527.44111	1527.44103	0.08
P5	1528.01428	1528.01421	0.07
P6	1528.59388	1528.59379	0.09
P10	1530.97621	1530.97616	0.05
P13	1532.83042	1532.83034	0.08
P14	1533.46131	1533.46125	0.06
P23	1539.42979	1539.42977	0.02
P24	1540.12535	1540.12528	0.07
P25	1540.82729	1540.82727	0.02

<sup>a</sup>Line center results for very-low-pressure conditions (less than 5 Pa). Our measurements (column 2) are values obtained by use of line centers at the different pressures extrapolated to zero pressure. Our expanded uncertainty for each line center is  $1 \times 10^{-4}$  nm (0.1 pm). The data in column 3 are from Ref. 3, measured at very low pressure with an estimated uncertainty of  $1.2 \times 10^{-6}$  nm.

**Table 4. Pressure Broadening Results<sup>a</sup>**

Line	Lorentzian Component of Linewidth (pm)			Linewidth Slope	
	6.7-kPa Cell	29.7-kPa Cell	66-kPa Cell	(pm/ kPa)	(MHz/ Torr)
R27	3.3(8)	13.3(8)	29.4(8)	0.44(2)	7.5(3)
R17	4.3	18.3	40.2	0.61	10.1
R11	4.9	22.6	50.2	0.76	13.0
R7	5.1	23.5	51.6	0.78	13.3
R1	6.1	25.2	55.8	0.84	14.3
P3	5.9	24.7	54.2	0.81	13.8
P4	5.6	23.5	51.9	0.78	13.3
P5	5.4	22.7	50.5	0.76	13.0
P6	5.3	-	48.1	0.72	12.3
P10	5.0	20.6	45.3	0.68	11.6
P13	4.9	20.6	44.9	0.67	11.4
P14	4.7	19.7	43.1	0.65	11.1
P23	3.9	15.7	34.4	0.51	8.7
P24	3.7	-	33.4	0.50	8.5
P25	3.6	15.6	32.3	0.48	8.2

<sup>a</sup>Width of the Lorentzian component of the Voigt line profile derived from fitting the lines with the Gaussian component, which is due to Doppler broadening, fixed at 3.7 pm. Results were obtained at the three pressures for selected lines of the  $\nu_1 + \nu_3$  band of acetylene  $^{12}\text{C}_2\text{H}_2$ . All the values in a column have the expanded uncertainty (coverage factor of 2) listed for the first value in the column.

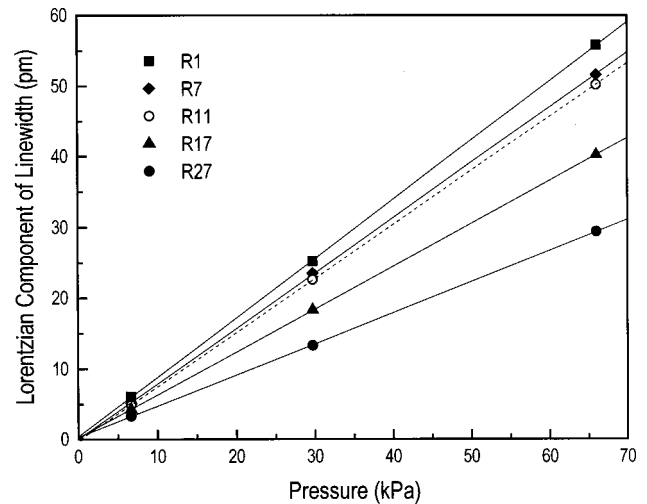


Fig. 6. Pressure broadening (Lorentzian component of the linewidth) for the measured lines in the  $^{12}\text{C}_2\text{H}_2$  R branch. Each line is shown with a linear least-squares fit to the data. The uncertainties are approximately the same size as the data points.

We attribute this result to the fact that the Voigt profile is generated numerically; small differences between algorithms can yield different model parameters. Since each line is a convolution of its Gaussian and Lorentzian components, the convolved linewidth at low pressure will be dominated by the width of the Gaussian component.

Our pressure broadening analysis does not include the small effect of collisional narrowing due to velocity averaging. This effect is negligible at higher pressures, where pressure broadening dominates, but can cause the line shape to deviate from the expected Voigt profile at low pressures.<sup>11</sup> Since we do not observe significant discrepancies between our data and the Voigt function, we conclude that the line-shape modification due to collisional narrowing is negligible at the level of our quoted uncertainty.

#### 4. SPECTRAL SENSITIVITY TO OTHER ENVIRONMENTAL CONDITIONS

Other environmental conditions can affect molecular spectra and can potentially shift line centers. For normal conditions, all these effects are small compared with the pressure shift and broadening described in Section 3. Below we discuss the effects of temperature variation and electromagnetic fields.

##### A. Temperature

Aside from the obvious effect that thermal distribution of population in rotational levels has on line strengths, thermally induced changes in molecular spectra are usually small for moderate temperatures. Moderate thermal changes can slightly modify the pressure shift and broadening of a molecular line by changing the collision frequency; both these collision-induced effects are proportional to the density of collision partners and their mean relative velocity.<sup>4</sup> In a closed cell containing only the gas phase, the density is fixed. The mean relative velocity is

proportional to the square root of the temperature. Thus the temperature dependence of the pressure shift,  $\Delta\nu(T)$ , is simply

$$\Delta\nu(T) = \Delta\nu(T_m)\sqrt{T/T_m}, \quad (2)$$

where  $\Delta\nu(T_m)$  is the pressure shift measured at temperature  $T_m$  and the temperatures  $T$  and  $T_m$  are in degrees Kelvin. From Eq. (2) it can be seen that the line center is fairly insensitive to temperature changes; a 50 K increase from room temperature would increase the pressure shift by only 8%. For the measurements reported here, the temperature was  $(22 \pm 2)^\circ\text{C}$ . This temperature range would cause a  $\pm 0.3\%$  change in the pressure shift, which is negligible compared with our other sources of uncertainty.

## B. Electromagnetic Fields

An excellent discussion of the effects of electromagnetic fields on molecular spectra can be found in Ref. 12. The ground state of acetylene and most other molecules is the  $^1\Sigma$  electronic state, where the angular momentum of the electronic cloud is zero. Consequently, magnetic field effects such as hyperfine structure (arising from the internal magnetic field) and the Zeeman effect (interaction of a magnetic moment with an external magnetic field) are much smaller than those normally found in atoms. This is simply due to the nature of the molecular chemical bond, where unpaired electrons in atoms pair up with electrons from another atom. Magnetic moments for these molecules are proportional to the overall rotational angular momentum and are  $\sim 1/1000$  that of an electron. Thus a moderately large magnetic field of 0.1 T (1000 G) would cause a Zeeman splitting of less than 1 MHz ( $\sim 0.01$  pm).

Electric quadrupole hyperfine structure (arising from the interaction of a nuclear electric quadrupole moment and the surrounding charge distribution) is absent in acetylene because it lacks a nuclear quadrupole moment. First- and second-order Stark shifts (arising from the interaction of the molecular electric dipole moment and an external electric field) are also absent; owing to its symmetry, the molecule has no permanent electric dipole moment. An electric field can polarize a molecule; this effect is  $\sim 10^4$  times smaller than second-order Stark effects and is therefore negligible, except in the case of extremely high electric fields.<sup>12</sup>

High-intensity ac electric fields can split and shift line centers.<sup>12</sup> This effect is referred to as the Autler–Townes effect, the ac Stark effect, or light shift and is significant when the laser intensity is comparable with the saturation intensity  $I_S$  of a transition. The saturation intensity has been estimated for line P13 of  $^{13}\text{C}_2\text{H}_2$  (Ref. 13) as  $I_S (\text{W/m}^2) = 15 \times 10^6 (0.1 + 10p)^2$  where  $p$  is the pressure in torr. For the lowest pressure used in our work (6.7 kPa = 50 Torr), this gives a saturation intensity of  $4 \times 10^8 \text{ W/cm}^2$ . Our measurements were made with an intensity of less than  $1 \text{ W/cm}^2$ , so we are clearly operating far from the regime in which this effect is significant. This effect may need to be taken into account for experiments done at low pressure and high intensity, such as those in which a power buildup cavity is used.

## 5. CONCLUSIONS

We have measured the pressure-induced shift for 15 lines of the  $\nu_1 + \nu_3$  rotational–vibrational band of acetylene  $^{12}\text{C}_2\text{H}_2$ . Although there is some variation with line number, over half the lines measured exhibit a shift near  $+0.017$  pm/kPa (or, equivalently,  $+2.3 \times 10^{-3}$  pm/Torr or  $-0.29$  MHz/Torr). We have also measured the pressure broadening of these lines and find that it also varies with line number and is typically  $\sim 0.7$  pm/kPa (12 MHz/Torr). For a pressure of 27 kPa ( $\sim 200$  Torr, the conditions of NIST Standard Reference Material 2517<sup>1</sup>), the line shift is typically near 0.5 pm but can be as large as 1.2 pm for lines far from the band center and can be as low as 0.2 pm for lines near the band center. The Lorentzian component of the linewidths at this pressure varies from 12 pm (1.5 GHz) for lines far from the band center to 23 pm (2.9 GHz) near the band center.

Although the pressure shift and the pressure broadening are both due to the interactions of molecules during collisions, they depend on line number rather differently. The pressure shift is largest for lines far from the band center (transitions between states with high rotational quantum number  $J$ ), whereas the pressure broadening is largest for lines near the band center (transitions between states with low  $J$ ). One explanation for the pressure broadening line dependence is that rotational averaging of the potential during a collision causes states with high rotational angular momentum (high  $J$ ) to be perturbed less than states with low  $J$ . The pressure shift is more difficult to interpret; it represents the difference between the shift of the excited state and the shift of the ground state. We would need to conduct a more extensive study before drawing any conclusions about the shift of a particular state. Measurements of the pressure broadening and the pressure shift of carbon monoxide lines<sup>14</sup> show trends that are very similar to those that we observe in acetylene.

We also evaluated the line sensitivity to temperature changes and to electromagnetic fields. We conclude that these effects are small compared with the collision-induced pressure broadening and pressure shift. In most cases thermal and electromagnetic effects can be neglected, although they can be significant at extreme temperatures and field strengths.

## ACKNOWLEDGMENTS

The authors are grateful to C. Wang for discussions and suggestions on the uncertainty analysis and to D. Nesbitt and L. Hollberg for discussions and comments on the manuscript.

S. Gilbert can be reached by e-mail at [sgilbert@boulder.nist.gov](mailto:sgilbert@boulder.nist.gov).

## REFERENCES

1. S. L. Gilbert, T. J. Drapela, and D. L. Franzen, "Moderate-accuracy wavelength standards for optical communications," in *Technical Digest—Symposium on Optical Fiber Measurements*, NIST Spec. Publ. 839 (National Institute of Standards and Technology, Boulder, Colo., 1992), pp. 191–194; S. L. Gilbert and W. C. Swann, "Acetylene  $^{12}\text{C}_2\text{H}_2$  ab-

- sorption reference for 1510–1540 nm wavelength calibration—SRM 2517,” NIST Spec. Publ. 260–133 (National Institute of Standards and Technology, Gaithersburg, Md., 1998).
2. S. L. Gilbert, W. C. Swann, and C. M. Wang, “Hydrogen cyanide  $\text{H}^{13}\text{C}^{14}\text{N}$  absorption reference for 1530–1560 nm wavelength calibration—SRM 2519,” NIST Spec. Publ. 260–137 (National Institute of Standards and Technology, Gaithersburg, Md., 1998).
  3. K. Nakagawa, M. de Labachellerie, Y. Awaji, and M. Kourogi, “Accurate optical frequency atlas of the 1.5- $\mu\text{m}$  bands of acetylene,” *J. Opt. Soc. Am. B* **13**, 2708–2714 (1996).
  4. W. Demtröder, *Laser Spectroscopy*, 2nd ed. (Springer-Verlag, Berlin, 1996), pp. 67–82.
  5. Y. Sakai, S. Sudo, and T. Ikegami, “Frequency stabilization of laser diodes using 1.51–1.55  $\mu\text{m}$  absorption lines of  $^{12}\text{C}_2\text{H}_2$  and  $^{13}\text{C}_2\text{H}_2$ ,” *IEEE J. Quantum Electron.* **28**, 75–81 (1992).
  6. B. N. Taylor and C. E. Kuyatt, “Guidelines for evaluating and expressing the uncertainty of NIST measurement results,” NIST Tech. Note 1297 (National Institute of Standards and Technology, Gaithersburg, Md., 1993).
  7. P. A. Boggs, R. H. Byrd, J. E. Rogers, and R. B. Schnabel, “User’s reference guide for ODRPACK version 2.01: software for weighted orthogonal distance regression,” NIST Interagency Rep. 4834 (National Institute of Standards and Technology, Gaithersburg, Md., 1992).
  8. A. Baldacci, S. Ghersetti, and K. N. Rao, “Interpretation of the acetylene spectrum at 1.5  $\mu\text{m}$ ,” *J. Mol. Spectrosc.* **68**, 183–194 (1977); G. Guelachvili and K. N. Rao, *Handbook of Infrared Standards II* (Academic, San Diego, Calif., 1993), pp. 564–571.
  9. G. P. Barwood, P. Gill, and W. R. C. Rowley, “Frequency measurements on optically narrowed Rb-stabilised laser diodes at 780 nm and 795 nm,” *Appl. Phys. B: Photophys. Laser Chem.* **53**, 142–147 (1991).
  10. J. Ye, S. Swartz, P. Jungner, and J. L. Hall, “Hyperfine structure and absolute frequency of the  $^{87}\text{Rb}$   $5\text{P}_{3/2}$  state,” *Opt. Lett.* **21**, 1280–1282 (1996).
  11. P. L. Varghese and R. K. Hanson, “Collisional narrowing effects on spectral line shapes measured at high resolution,” *Appl. Opt.* **23**, 2376–2385 (1984).
  12. C. H. Townes and A. L. Schawlow, *Microwave Spectroscopy* (Dover, New York, 1975), Chaps. 10 and 11.
  13. M. de Labachellerie, K. Nakagawa, and M. Ohtsu, “Ultra-narrow  $^{13}\text{C}_2\text{H}_2$  saturated-absorption lines at 1.5  $\mu\text{m}$ ,” *Opt. Lett.* **19**, 840–842 (1994).
  14. J. Henningsen, H. Simonsen, T. Møgelberg, and E. Trudsó, “The  $0 \rightarrow 3$  overtone band of CO: precise linestrengths and broadening parameters,” *J. Mol. Spectrosc.* **193**, 354–362 (1999).